REPRODUCTION
RESEARCH

Cytotoxic effects of Shiga toxin-2 on human extravillous trophoblast cell lines

María Luján Scalise[1], María Marta Amaral[1], Julieta Reppetti[2], Alicia E Damiano[2,3], Cristina Ibarra[1] and Flavia Sacerdoti[1]

[1]Laboratorio de Fisiopatogenia, Departamento de Ciencias Fisiológicas, Instituto de Fisiología y Biofísica (IFIBIO) Houssay, Facultad de Medicina, Universidad de Buenos Aires, Buenos Aires, Argentina, [2]Laboratorio de Biología de la Reproducción, Departamento de Ciencias Fisiológicas, Instituto de Fisiología y Biofísica (IFIBIO) Houssay, Facultad de Medicina, Universidad de Buenos Aires, Buenos Aires, Argentina and [3]Cátedra de Biología Celular y Molecular, Departamento de Ciencias Biológicas, Facultad de Farmacia y Bioquímica, Universidad de Buenos Aires, Buenos Aires, Argentina

Correspondence should be addressed to F Sacerdoti; Email: flasacerdoti@gmail.com

Abstract

Shiga toxin (Stx2) producing *Escherichia coli* infections during early gestation may impair placentation through a Stx2 damage of extravillous trophoblast (EVT) cells. We have previously demonstrated that Stx2 injected in rats in the early stage of pregnancy causes spontaneous abortion by a direct cytotoxic effect in the highly perfused feto-uteroplacental unit. The main aim was to evaluate the effects of Stx2 on EVT in order to understand the possible adverse effects that the toxin may have on trophoblast cells during early pregnancy. Swan 71 and HTR-8 cell lines were used as human EVT models. The presence of Stx2 receptor, globotriaosylceramide (Gb3), on Swan 71 and HTR-8 cells was evaluated by thin layer chromatography. The effects of Stx2 on cell viability were evaluated by neutral red uptake, migration by wound-healing assay and invasion was determined by the 'transwell chamber' assay. Metalloproteinase activity (MMP-2) was evaluated by zymography and tubulogenesis was analyzed by counting the total tube length and the number of branch formation. We have demonstrated that Swan 71 expresses high levels of Gb3 compared to HTR-8 cells. Stx2 decreased significantly Swan 71 viability in a dose-dependent manner after 72 h of toxin exposure. Furthermore, Stx2 impaired migration, invasion and tube-like formation of Swan 71 cells and decreased the MMP-2 activity. These cytotoxic effects were partially prevented by aminoguanidine, an inducible nitric oxide synthase inhibitor. These studies demonstrate that the function and viability of EVT cells may be altered by Stx2 and suggest that NO overexpression may be involved in the detrimental effects.
Reproduction (2019) **157** 297–304

Introduction

Shiga toxin type 2 (Stx2) is the main virulence factor of Shiga toxin producing *Escherichia coli* (STEC). STEC are gastrointestinal bacteria whose infection can cause diarrhea, hemorrhagic colitis and hemolytic uremic syndrome (HUS). STEC are present in the intestinal tract of healthy cattle, and transmission to humans occurs by consumption of undercooked ground beef, manure-contaminated water, vegetables and by direct transmission from person to person (Hussein 2007).

After the ingestion of bacteria, STEC colonizes the human intestine where Stx is released and crosses the intestinal mucosal barrier. Then, the toxin circulates in the bloodstream and reaches its target organs, mainly kidneys and brain (Ibarra *et al.* 2013). Stx has an AB_5 molecular configuration where an enzymatically active monomeric A subunit is non-covalently associated with a pentamer of B subunit which is responsible for binding to globotriaosylceramide (Gb3) receptor (Waddell *et al.* 1990). Gb3 is located on the plasma membrane of target cells, particularly endothelial cells present in kidneys, brain and other organs (Obrig *et al.* 1993, Muthing *et al.* 2009). The binding of Stx to Gb3 is the primary determinant of its cytotoxic effects and results in toxin internalization and cell death by the inhibition of protein synthesis and induction of apoptosis (Bergan *et al.* 2012). Post-enteric HUS is a systemic complication of STEC infection characterized by hemolytic anemia, thrombocytopenia and acute renal failure, and is caused principally by the effects of Stx on the target organs (Karmali *et al.* 1985).

Infections during pregnancy have been widely associated with adverse pregnancy outcomes, including premature delivery, premature rupture of membranes and miscarriage (Gibbs 2001). The pathogens most frequently associated with preterm labor and delivery are clearly identifiable in over 30% of cases. The organisms most commonly associated with preterm

ISSN 1470–1626 (paper) 1741–7899 (online)
https://doi.org/10.1530/REP-18-0581
Online version via https://rep.bioscientifica.com

labor include *Ureaplasma urealyticum, Mycoplasma hominis, Streptococcus agalactiae* and *Escherichia coli* (Peltier 2003). Besides, many causes of pregnancy complications are often unknown, and have not yet been investigated. During early pregnancy, trophoblasts are the outermost cell layer of the blastocyst. Once attached onto the uterine wall, trophoblasts differentiate into two different types: cytotrophoblast and syncytiotrophoblast and further, cytotrophoblast gives rise to the extravillous (EVT) and villous (VT) trophoblast populations. EVT cells invade and proliferate into the decidua to develop the placenta and VT cells fuse to form a syncytium that comprise the placental barrier between the maternal and fetal circulation. Failed invasion by EVT is associated with early pregnancy loss and adverse obstetric, such as preeclampsia or intrauterine growth restriction (Brosens *et al.* 2011). Clinically, most of pregnancy losses are not studied, unless they are recurrent, and it is unknown whether STEC infection can effectively affect human early pregnancy. In contrast, experimental *in vivo* animal models have demonstrated that bacteria and bacterial products may trigger preterm delivery and pregnancy loss mediated by proinflammatory cytokines. Increased production of proinflammatory cytokines including TNF-α and IL-1β triggers production of free radicals such as nitric oxide (NO) (Sprague & Khalil 2009). NO is a signaling molecule with several biological activities, including vasodilatation, neurotransmission, immunomodulation and antimicrobial. NO is formed from L-arginine by the enzyme nitric oxide synthase. This enzyme exists as three isoforms: calcium-dependent isoforms originally characterized in neuronal tissue (nNOS), the constitutively expressed endothelial isoform (eNOS) and the inducible isoform (iNOS) mainly induced in cells of the innate immune system such as macrophages and neutrophils. eNOS and iNOS have been reported to be present in human placenta (Hambartsoumian *et al.* 2001). Furthermore, inhibitors of iNOS block lipopolisaccharide (LPS)-induced preterm labor in mice, reduced peroxynitrite formation and prevented apoptosis in human trophoblasts cell (Athanassakis *et al.* 1999, Asagiri *et al.* 2003). NO role during early pregnancy is believed to contribute to maintenance of low vascular resistance in the fetoplacental circulation, contributing to spiral artery remodeling and myometrial quiescence. In this sense, continuous production of NO by trophoblast cells reaches high importance during the early stages of pregnancy (Al-Hijji *et al.* 2003).

We have previously demonstrated that Stx2 injected in rats in the late stage of pregnancy induces premature delivery of dead fetuses (Burdet *et al.* 2009), and additionally, in the early stage of pregnancy causes spontaneous abortion by a direct cytotoxic effect in the highly perfused feto-uteroplacental unit (Sacerdoti *et al.* 2014). Dissemination of Stx2 into the peripheral blood during early pregnancy may expose the placenta to infection. Gb3 receptor of Stx2 has been detected in placental tissue (Strasberg *et al.* 1989) but the direct effects of the Stx2 in trophoblast cells have not been investigated yet.

Therefore, the hypothesis of our research is that Stx2 can alter the correct invasion of trophoblast cell during early gestation and impairs the development of the placenta. The main aim was to evaluate the effects of Stx2 on EVT in order to understand the possible adverse effects that the toxin may cause on trophoblast cells during early pregnancy.

Materials and methods

Drugs and chemicals

Toxins: Shiga toxin type 2 (Stx2) was purchased from Phoenix Laboratory (Tutfs Medical Center, Boston, MA, USA) and was checked for LPS contamination by the Limulus amoebocyte lysate assay, BioWhittaker Inc. (Maryland, USA). Gb3 standard was purchased from Matreya (Pleasant Gap, PA, USA). Reagents for thin layer chromatograph were provided by Aberkon Quimica and Sintorgan S.A (Buenos Aires, Argentina). DAPI (4′,6-diamidino-2-phenylindole) was purchased from Sigma-Aldrich (USA). Aminoguanidine (AG) was supplied by Sigma-Aldrich (USA). Extracellular matrix gel from Engelbreth-Holm-Swarm murine sarcoma gel (Matrigel) was provided by Sigma-Aldrich (Buenos Aires, Argentina).

Cell lines culture

Human extravillous trophoblast (EVT) Swan 71 cell line derived by telomerase-mediated transformation of a 7-week cytotrophoblast isolate was kindly provided by Dr. Gil Mor, Yale University, New Haven, CT, USA (Straszewski-Chavez *et al.* 2009). Swan 71 cells were cultured in Dulbecco's Modified Eagle Medium/Nutrient Mixture F-12 (DMEM F-12, Sigma-Aldrich, USA).

Human EVT HTR-8/SVneo cell line (HTR-8) obtained from explant cultures of human first trimester placenta (8 to 10 weeks of gestation) was immortalized by transfection with a cDNA construct that encodes the SV40 large T antigen kindly provided by Dr. Udo Markert, Placenta Lab, Department of Obstetrics, Jena University Hospital, Jena (Graham *et al.* 1993). HTR-8 cells were cultured in Roswell Park Memorial Institute (RPMI-1640; Sigma-Aldrich, USA).

Vero cell line (Vero) derived from African green monkey kidney was purchased from American Type Culture Collection (ATCC-CCL 81, Manassas, VA) and cultured in RPMI-1640 medium (Sigma-Aldrich, USA). All media were supplemented with 10% fetal calf serum (FCS), (Internegocios S.A., Buenos Aires, Argentina), 100 U/mL penicillin/streptomycin, (GIBCO, USA) and 2 mM L-glutamine at 37°C in a humidified 5% CO_2 incubator. For growth-arrested conditions, medium without FCS was used.

Thin layer chromatography (TLC)

The presence of the Stx2 receptor, globotriaosylceramide (Gb3), on Swan 71 and HTR-8 cells was evaluated by TLC. Total cell glycolipids were extracted from 2×10^6 cells according to the method of Bligh and Dyer as discussed previously (Bligh & Dyer 1959). Briefly, 3 mL of a chloroform:methanol (2:1 v/v) mixture was added to the cells and incubated on ice for 15 min. Then 2 mL of chloroform:water (1:1) mixture was added to the tube and centrifugated at 3000 rpm for 5 min to separate phases. The aqueous phase was discarded and the organic phase with extracted lipids was allowed to air-dry. One mL of methanol and 0.1 mL of 1 M NaOH were added to the dried residue and the mixture was incubated for 24 h at 37°C. Finally, 2 mL of chloroform and 0.5 mL water were added, phases were separated by centrifugation and the upper phase was removed. The lower phase, corresponding to glycolipid extract, was brought to dryness. Fractionated lipids were subjected to TLC with a silica gel (Aluminum plate, 60, F254, Merck, Germany) previously activated by incubation for 15 min at 100°C. Glycolipids were separated in a glass tank with a mixture of chloroform/methanol/water (65:35:8). A purified Gb3 standard was added to the plate for comparison. After the solvent front reached the top of the plate, the silica plate was air dried and treated with a solution of orcinol (50 mg orcinol, 10 mL of sulfuric acid and 39.5 mL of water) to visualize the separated neutral glycolipids. Densitometric analysis of Gb3 band was performed with ImageJ software (NIH, USA). Gb3 content in each cell type was calculated comparing with Gb3 standard band intensity.

Neutral red viability assay

The neutral red cytotoxicity assay was adapted from previously described protocols (Creydt *et al.* 2006). Briefly, $1.8\,10^4$ EVT cells (Swan 71 or HTR-8) were seeded in 96-well plates and grown to 80% of confluence. The cells were then washed with PBS and exposed to different concentrations of Stx2 (1×10^{-7}–1 µg/mL) in growth-arrested conditions for 24 and 72 h. After treatment, cells were incubated with neutral red (50 µg/mL) for an additional 1 h at 37°C in 5% CO_2. Cells were then washed and fixed with 200 µL of 1% $CaCl_2$/1% formaldehyde and then lysed with a solution of 1% acetic acid in 50% ethanol to solubilize the neutral red. Absorbance in each well was read at 540 nm in an automated plate spectrophotometer (RT-6000, Rayto Life and Analytical Sciences Co. Ltd., China). Results are expressed as percentage of cell viability where 100% represents control cells under identical conditions without toxin treatment. The 50% cytotoxic dose (CD_{50}) represents the dilution required to kill 50% of cells.

Wound-healing assay

Swan 71 (5×10^4 cells/well) were plated in 24-well culture dishes and incubated at 37°C and 5% of CO_2 until 80% confluence in complete DMEM/F12 medium. The cells were then treated with different concentrations of Stx2 (0.001–1 µg/mL), 100 µM AG or a combination of 0.1 µg/mL Stx2 and 100 µM AG (Stx2 + AG) for 24 h in growth-arrested conditions. After treatment, a vertical scratch was performed in the center of each well with a 200 µL sterile pipette tip and cell debris was then removed by washing the wells twice with PBS (Alejandra *et al.* 2018). Then, DMEM F-12 medium (500 µL) was added to each well and cells were cultured for 24 h at 37°C with 5% CO_2. Images of the wound were taken at the initial wounding ($t = 0$ h) and after 24 h ($t = 24$ h) with a digital camera (Micrometrics 591CU CCD 5.0 Megapixel Camera) in a phase-contrast microscope (Nikon Eclipse T2FL, USA). The ratio of the final area relative to the initial wound area was calculated and quantified using TScratch software version 1.0. Results are expressed as % of wound closure (wound area at 24 h – wound area at 0 h). All the experiments were performed three times.

Transwell invasion assay

Invasion assay was performed in transwell (8 µm pore size; Corning Life Sciences), coated with Matrigel. Briefly, diluted 1:10 Matrigel (11 mg/mL) in DMEM-F12 was added to the upper side of the insert on a 24-well transwell plate, and incubated at 37°C for 2 h for solidification. Swan 71 cells (4×10^4 cells/well) were then added to the upper side of the insert in 250 µL of DMEM-F12 without FCS and incubated with different concentrations of Stx2 (0.01–1 µg/mL), 100 µM AG or a combination of 0.1 µg/mL Stx2 and 100 µM AG (Stx2 + AG). Additionally, 500 µL of DMEM-12 medium was added to the lower side of the well. Then cells were incubated for 24 h in a incubator (37°C, 5% CO_2). After incubation, the cells on the Matrigel side of the inserts were then removed with cotton swab and the inserts were fixed in methanol and stained with DAPI (0.5 µg/mL in PBS). Then, the stained nuclei were observed with a fluorescence microscope (Nikon Eclipse 200, NY, USA) and the number of invading cells was calculated by counting the total number of stained nuclei in photographs of ten random fields (×200) for each experimental condition. The experiment was performed three times.

Gelatin zymography

Matrix metalloproteinase-2 activity (MMP-2) in Swan 71 was analyzed by gelatin zymography. For that purpose, Swan 71 cells were seeded on 24 plate (1×10^4 cells/well) wells and incubated for 24 h with different concentrations of Stx2 (0.01–1 µg/mL) or without toxin for control. Cell supernatants were collected after 24, 48 and 72 h. Samples were stored at −20°C until gelatin zymography was performed. For each condition, the protein concentration was determined with the BCA Protein Assay Kit (Pierce Biotech. Inc). Then, equal amounts of protein (60 µg) of each experimental condition were loaded in each line of a 7.5% polyacrylamide gel (SDS-PAGE) containing 1 mg/mL gelatin (Sigma-Aldrich, USA). After electrophoresis (100V constant), the gels were soaked in 2.5% Triton X-100 for 30 min to remove SDS and incubated for 48 h at 37°C in zymography Tris buffer (50 mM Tris-HCl, 120 mM NaCl, 5 mM $CaCl_2$, 5 µM $ZnCl_2$, pH 7.8). Gels were then stained with 0.1% Coomassie blue in 50% methanol and 15% acetic acid, and then washed with 10% acetic acid to individualize the zones with gelatinase activity. Areas

where gelatin was degraded were seen as clear bands. Band intensities were quantified using ImageJ software (NIH, USA) and compared to control.

Tube-like formation assay

In order to analyze the action of Stx2 on Swan 71 tube-like formation, cells were grown in 6-well culture dishes (1×10^5 cell/well) at 37°C and 5% of CO_2 until 80% confluence and incubated for 24 h with different concentrations of Stx2 (0.01–1 µg/mL), 100 µM AG or a combination of 0.1 µg/mL Stx2 and 100 µM AG (Stx2 + AG). Then, cells were seeded in 96-well plates (1.8×10^4 cell/well) coated with Matrigel (40 µL, 11 mg/mL) and incubated at 37°C with 5% CO_2 in DMEM/F12 medium without FCS. Six hours after culture tube-like formation was observed in an inverted light microscope and five random fields were photographed with a digital camera (Nikon Eclipse T2FL, USA). Extreme edges were excluded due to gel meniscus formation. ImageJ software (NIH, USA) with plugin *angiogenesis analyzer* was used to quantify the total tube length in pixel and branches (number of branches of the analyzed area) formation of each condition. The experiments were performed three times.

Statistical analysis

Statistical analysis was performed using the GraphPad Prism Software 5.0 (San Diego, CA, USA). Analysis of variance (one-way ANOVA) was used to calculate differences between groups and Tukey's was used as *a posteriori test*. Statistical significance was set at $^*P < 0.05$.

Results

Gb3 expression and Stx2 cytotoxic effects on EVT

In order to determine the presence of Gb3 receptor in Swan 71 and HTR-8 cells, the neutral glycolipids extracted from 1×10^6 cells were subjected to TLC and then visualized with orcinol staining. A commercial Gb3 (1 µg/lane) was used as standard and Vero cells were used as a positive control. Two bands located at the same distance of Gb3 standard were found in Swan 71 cells with an intensity comparable to the bands observed in Vero cells (Fig. 1A). In contrast, HRT-8 cells showed a substantially lower expression of Gb3 compared to Swan 71 cells. Semi-quantitative analysis of Gb3 bands by densitometry showed that Swan 71 express a significantly higher level of Gb3 receptor than HRT-8 cells (Fig. 1B).

The cytotoxic effects of Stx2 on trophoblast cells were evaluated by viability assay using neutral red uptake. Stx2 decreased significantly the cell viability in a dose-dependent manner of Swan 71 but not of HTR-8 cells after 72 h of toxin exposure (Fig. 1C). Stx2 cytotoxicity on Swan 71 cells was also dependent on the time of exposure to the toxin, since these cells showed no cytotoxic effects after 24 h of incubation with Stx2 (Fig. 1C).

Stx2 inhibits Swan 71 cell migration

To evaluate the impact of Stx2 on extravillous trophoblast cell migration, Swan 71 cells were grown at 80% of confluence in 24-well plates and incubated for 24 h with or without Stx2 (0.001–1 µg/mL). Then a wound in the center of each well was made and images were obtained at 0 and 24 h after wound healing (Fig. 2A). Treatment of Swan 71 cells with 0.1 and 1 µg/mL of Stx2 showed a significant reduction of trophoblast migration (37 ± 6% and 43 ± 10%, respectively) compared to control (Fig. 2B).

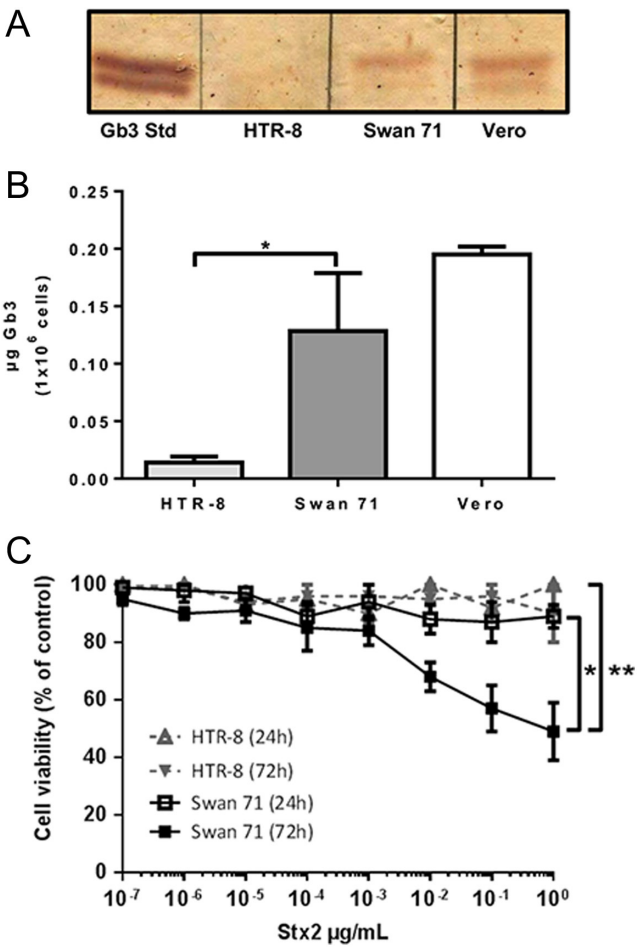

Figure 1 Gb3 expression on trophoblast cells and Stx2 cytotoxic effects. (A) Neutral glycolipids extracted from HTR-8, Swan 71 and Vero cells were subjected to TLC and then visualized with orcinol staining. (B) Gb3 glycolipid bands from 1×10^6 cells were quantified by densitometric analysis and compared to standard Gb3 (1 µg/lane, Matreya). (C) Cells were exposed to different concentrations of Stx2 (1×10^{-7}–1 µg/mL) in growth-arrested conditions for 24 and 72 h. Then, cells were incubated with neutral red for an additional 1 h. Results are expressed as percentage of cell viability where 100% represents control cells without toxin treatment. Data are shown as means ± S.D. from at least five independent experiments performed in triplicate. $^*P < 0.05$ for Swan 71 (72 h) vs Swan 71 (24), $^{**}P < 0.01$ for Swan 71 (72 h) vs HRT-8 (24 h) and HTR-8 (72 h).

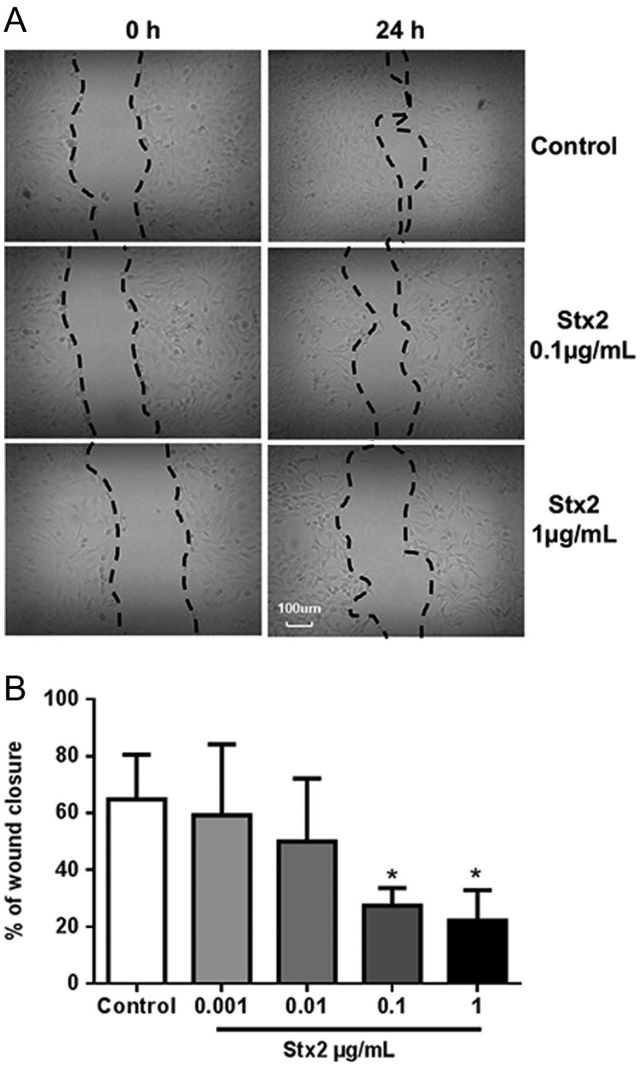

Figure 2 Stx2 inhibits trophoblast cell migration. (A) Cell migration was evaluated in Swan 71 cells by the wound-healing assay in cells grown in 24-well plates and incubated for 24 h with Stx2 (0.001–1 µg/mL) before wound formation. Images of the wound healing were captured at 0 h and 24 h using a light microscope (×200) (B) Cell migration was calculated and expressed as percentages of cell coverage to the initial cell-free zone. Values are presented as means ± S.D. Experiments were repeated three times. Significant differences (*$P < 0.05$) were found compared to the control.

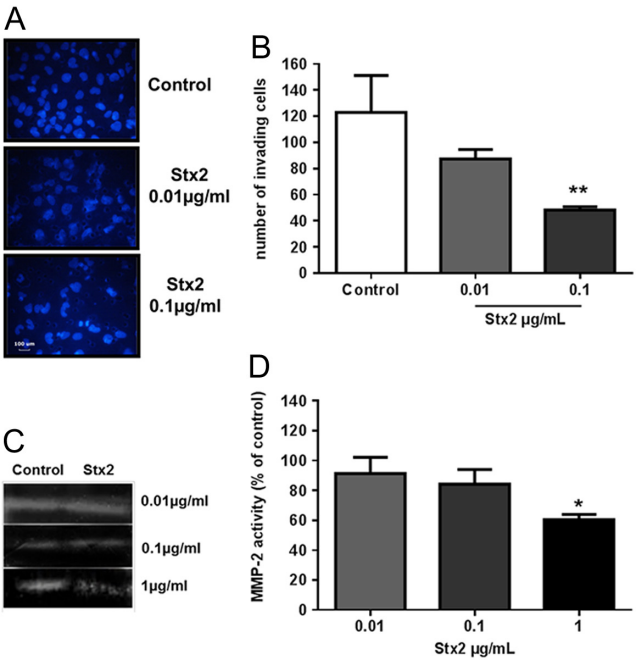

Figure 3 Stx2 inhibits trophoblast cell invasion and MMP-2 activity. Swan 71 cells were grown on transwell insert (8 µm pore size) coated with 0.5 mg/mL Matrigel (Sigma) and incubated for 24 h with Stx2 (0.01 and 0.1 µg/mL). Cells that invaded the lower side of the insert were fixed with methanol and stained with DAPI. (A) Representative photographs of invading cells in each experimental condition (×200). (B) Stx2 at 0.1 µg/mL significantly decreased Swan 71 cell invasion compared to control. MMP-2 activity was evaluated by zymography assay in Stx2-treated and non-treated Swan 71 cells incubated with Stx2 for 24 h. (C) a representative zymography is shown. (D) The densitometric analysis of MMP-2 band intensity showed a significant decrease of MMP-2 activity on Stx2 treated compared to control. Values are presented as means ± S.D. Each experiment was repeated three times. *$P < 0.05$.

Stx2 reduces Swan 71 cell invasion

The effects of Stx2 on the invasive capacity of Swan 71 cells was evaluated by the transwell invasion assay (Fig. 3A). The number of invading cells decreased in Swan 71 cells treated with 0.01 and 0.1 µg/mL Stx2 (29 ± 8% and 66 ± 5%, respectively) compared to control (Fig. 3A and B). Taking into account that metalloproteinases are critical for trophoblast invasion and migration due to their degrading properties of the extracellular matrix, the effects of Stx2 on the activity of MMP-2 in Swan 71 cells at 24 h was evaluated by zymography assay. The densitometric analysis of MMP-2 band intensity showed a significant decrease in Swan 71 cells treated with 1 µg/mL Stx2 compared with control cells (Fig. 3C and D).

Stx2 inhibits tube-like formation

A significant decrease of the tube-like formation was detected in Swan 71 cells treated with different Stx2 concentrations. The total tube length and branch formations was inhibited by Stx2 in a dose-dependent manner (Fig. 4B and C). These results show that Stx2 impairs trophoblast tube-like formation at a shorter time (6 h) compared to that needed to affect cell viability (72 h, Fig. 1C).

AG partially prevents Stx2 effects on Swan 71 cells

In order to assess the possible deleterious mechanisms triggered by Stx2, and the role of NO in these effects, Swan 71 cells were treated with 100 µM AG concomitantly with 0.1 µg/mL Stx2. AG partially prevented the cytotoxic

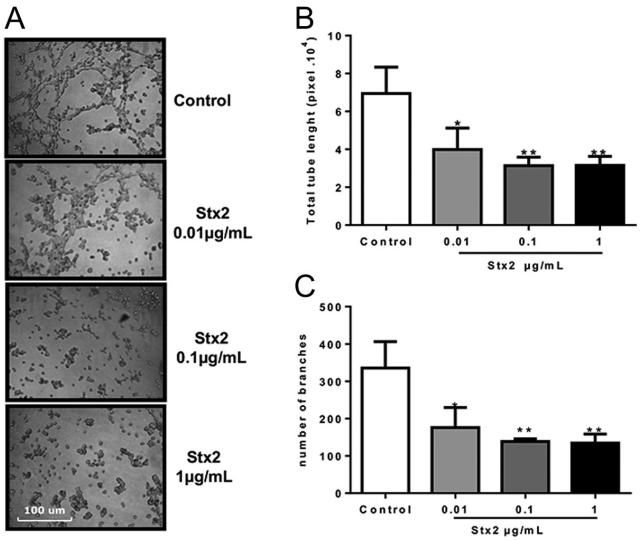

Figure 4 Stx2 inhibits tube-like formation of trophoblast cells. Swan 71 cell monolayers treated with Stx2 were seed in 96-well plates coated with Matrigel. Pictures were taken of ten random fields 6 h after tube-like formation (×100). (A) Representative images of tube-like formation. (B) Total tube length and (C) number of branches were quantified in control and Stx2-treated cells. Stx2 significantly decreases each one of the parameters involved in tube-like formation compared to control. Values are presented as means ± S.D. Each experiment was repeated three times. *$P<0.05$, **$P<0.01$.

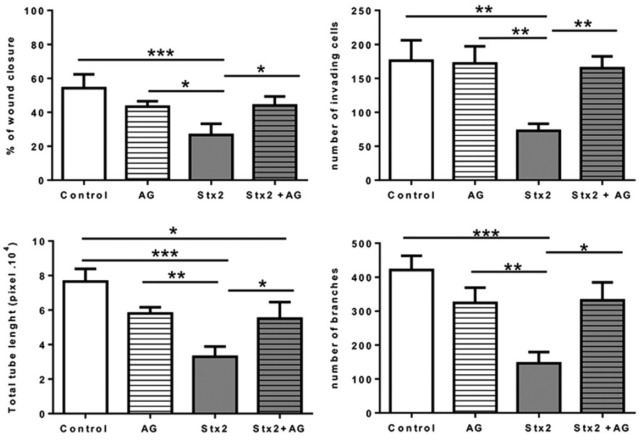

Figure 5 Aminoguanidine (AG) partially prevents Stx2 effects on trophoblast cells. AG (100 µM) partially prevented the cytotoxic effects of Stx2 (0.1 µg/mL) on (A) migration, (B) invasion and (C) total tube length and (D) number of branches of Swan 71 cells. Data are shown as means ± S.D. from at least three independent experiments. *$P<0.05$; **$P<0.01$, ***$P<0.001$.

Stx2 effects on migration (Fig. 5A), invasion (Fig. 5B) and tube-like formation (total tube length and number of branch formations) (Fig. 5C and D).

Discussion

During human placentation, EVT cells migrate and invade the maternal decidua and acquire an endovascular phenotype in order to reconstruct maternal spiral arteries to facilitate supply of the nutrients and oxygen to the developing fetus (Staun-Ram & Shalev 2005). Thus, EVT functions are extremely regulated and coordinated and are crucial for a correct placentation (Cartwright & Whitley 2017). It's also well known that infections during pregnancy are associated with adverse outcomes including miscarriage, premature rupture of membranes, preterm birth, growth restriction and still birth (Giakoumelou *et al.* 2016). In this sense, virulence factors secreted by pathogens may also impair the correct placentation. STEC are foodborne bacteria that, once ingested, colonize the intestine and promote the production and absorption of Stx responsible for triggering cell death in target organs (Torres 2017). We propose that Stx may mediate EVT impairment leading to pregnancy complications. In this regard, we have previously reported that Stx2 induces disruption of placental tissues and produces a significant hypoxic environment in the implantation site, intrauterine hemorrhage, and neutrophil infiltration and finally causes early pregnancy loss in rats. Stx2 effects observed in rats were proposed to be a consequence of a direct action of Stx2 on the feto-placental unit (Sacerdoti *et al.* 2015). In the present study, we aimed to gain insight into the effects of Stx2 on human EVT. Taking into account that it is difficult to obtain human tissues from the first trimester of pregnancy and keep them in the long term, several immortalized trophoblast cell lines with phenotypic and functional characteristics similar to normal human EVT were used as human EVT models. However, there are still controversies about which cell line represents better *in vivo* cells (Bilban *et al.* 2010). Our work showed that Stx2 decreases significantly Swan 71 viability in a dose- and time-dependent manner but do not affect HTR-8 viability. We hypothesize that differences on the cytotoxic action of Stx2 between both cell lines may be due to a higher expression of Gb3 receptor on Swan 71 compared to HTR-8 detected by TLC. In this sense, several studies have demonstrated that Stx cytotoxicity is associated with the presence of Gb3 receptor and that binding of Stx to Gb3 is the primary event to trigger death of endothelial and epithelial cells (Bauwens *et al.* 2013, Melton-Celsa 2014). Herein, we have demonstrated that Gb3 expression is higher in Swan 71 than HTR-8 cells and this additional feature was taken into account when Swan 71 cell line was chosen for our studies.

It has been well described that Stx2 after binding to Gb3 takes a retrograde transport through Golgi and the endoplasmic reticulum where an active A subunit of the toxin is released to the cytosol and produces the inhibition of ribosomes leading to a ribotoxic stress and cell death (Bergan *et al.* 2012). Interestingly, our results demonstrated that Stx2 impairs migration, invasion and tube-like formation of Swan 71 cells at lower doses compared to those that produce cell death. This

difference may indicate that even if no cell death is observed, Stx2 may impair molecular mechanisms that damage cell functionality. Migration and invasion of EVT are processes finely regulated by many autocrine and paracrine growth factors and the extracellular matrix components among others (Lala & Chakraborty 2003). Moreover, a reduction on MMP-2 activity by Stx2 suggests that the inhibition of this gelatinase may be, at least in part, responsible for these Stx2 effects. Disruption of trophoblast functionality by Stx2 may cause irreversible damages in pregnancy and failure on EVT invasion could be associated with complications such as intrauterine growth restriction, preeclampsia, premature delivery or miscarriage (Tang *et al.* 2017).

In normal conditions, NO is the main vasodilator in the placenta and is crucial for the maintenance and control of fetoplacental hemodynamics. It has been well described that eNOS and iNOS are involved in the NO production (Forstermann & Sessa 2012). Altered levels of placental NO could explain the vascular dysfunction in several pregnancy pathologies (Krause *et al.* 2011). Additionally, Asagiri *et al.* (2003) demonstrated that peroxynitrites are involved in the trophoblastic apoptosis triggered by LPS. These authors also reported that NO inhibitors can be candidate therapeutic agents for infectious diseases, which are associated with overproduction of NO. In this work, we have shown that the impairment of migration, invasion and tube-like formation caused by Stx2 can be partially prevented by AG suggesting that overexpression of NO may be, in part, involved in the detrimental Stx2 effects on EVT as we previously described in rats in the late stage of pregnancy (Burdet *et al.* 2010).

This study is the first to report that the function and viability of EVT cells are altered by Stx2 and suggest that NO overexpression may be involved in the detrimental effects. We thus speculate that an infection by STEC during first trimester of pregnancy may induce placental dysfunction. Altogether we propose that STEC infection during early pregnancy could damage human trophoblast by a direct action of Stx2 (Sacerdoti *et al.* 2018). Further epidemiological studies about the prevalence of symptomatic or asymptomatic STEC infections in pregnant women will help to understand the role of STEC infections during pregnancy.

Declaration of interest

The authors declare that there is no conflict of interest that could be perceived as prejudicing the impartiality of the research reported.

Funding

This research did not receive any specific grant from any funding agency in the public, commercial or not-for-profit sector.

Author contribution statement

M L Scalise contributed to the concept and design, interpreted and analyzed the data, supplied statistical expertise, collected and assembled the data. J Reppetti and M M Amaral interpreted and analyzed the data. A E Damiano, C Ibarra and F Sacerdoti contributed to the concept, assembled the data, provided drafting of the article and obtained a funding source.

Acknowledgements

Parts of these results were presented at the 10th International Symposium on Shiga toxin (Verocytotoxin) producing *Escherichia coli* infection (VTEC2018), Florence, Italy, 6–9 May 2018. We thank Natalia Beltramone and Analía López Díaz for their excellent technical assistance. This work was supported by research grants from FONCyT (PICT 2014-0937, F S, M M A and C I; 2016-292, A E D and C I) and the University of Buenos Aires (UBACYT-2014, F S, M M A, C I).

References

Alejandra R, Natalia S & Alicia ED 2018 The blocking of aquaporin-3 (AQP3) impairs extravillous trophoblast cell migration. *Biochemical and Biophysical Research Communications* **499** 227–232. (https://doi.org/10.1016/j.bbrc.2018.03.133)

Al-Hijji J, Andolf E, Laurini R & Batra S 2003 Nitric oxide synthase activity in human trophoblast, term placenta and pregnant myometrium. *Reproductive Biology and Endocrinology* **1** 51. (https://doi.org/10.1186/1477-7827-1-51)

Asagiri K, Nakatsuka M, Konishi H, Noguchi S, Takata M, Habara T & Kudo T 2003 Involvement of peroxynitrite in LPS-induced apoptosis of trophoblasts. *Journal of Obstetrics and Gynaecology Research* **29** 49–55. (https://doi.org/10.1046/j.1341-8076.2003.00066.x)

Athanassakis I, Aifantis I, Ranella A, Giouremou K & Vassiliadis S 1999 Inhibition of nitric oxide production rescues LPS-induced fetal abortion in mice. *Nitric Oxide* **3** 216–224. (https://doi.org/10.1006/niox.1999.0224)

Bauwens A, Betz J, Meisen I, Kemper B, Karch H & Muthing J 2013 Facing glycosphingolipid-Shiga toxin interaction: dire straits for endothelial cells of the human vasculature. *Cellular and Molecular Life Sciences* **70** 425–457. (https://doi.org/10.1007/s00018-012-1060-z)

Bergan J, Dyve Lingelem AB, Simm R, Skotland T & Sandvig K 2012 Shiga toxins. *Toxicon* **60** 1085–1107. (https://doi.org/10.1016/j.toxicon.2012.07.016)

Bilban M, Tauber S, Haslinger P, Pollheimer J, Saleh L, Pehamberger H, Wagner O & Knofler M 2010 Trophoblast invasion: assessment of cellular models using gene expression signatures. *Placenta* **31** 989–996. (https://doi.org/10.1016/j.placenta.2010.08.011)

Bligh EG & Dyer WJ 1959 A rapid method of total lipid extraction and purification. *Canadian Journal of Biochemistry and Physiology* **37** 911–917. (https://doi.org/10.1139/o59-099)

Brosens I, Pijnenborg R, Vercruysse L & Romero R 2011 The 'Great Obstetrical Syndromes' are associated with disorders of deep placentation. *American Journal of Obstetrics and Gynecology* **204** 193–201. (https://doi.org/10.1016/j.ajog.2010.08.009)

Burdet J, Zotta E, Franchi AM & Ibarra C 2009 Intraperitoneal administration of Shiga toxin type 2 in rats in the late stage of pregnancy produces premature delivery of dead fetuses. *Placenta* **30** 491–496. (https://doi.org/10.1016/j.placenta.2009.03.012)

Burdet J, Zotta E, Cella M, Franchi AM & Ibarra C 2010 Role of nitric oxide in Shiga toxin-2-induced premature delivery of dead fetuses in rats. *PLoS One* **5** e15127. (https://doi.org/10.1371/journal.pone.0015127)

Cartwright JE & Whitley GS 2017 Strategies for investigating the maternal-fetal interface in the first trimester of pregnancy: what can we learn about pathology? *Placenta* **60** 145–149. (https://doi.org/10.1016/j.placenta.2017.05.003)

Creydt VP, Silberstein C, Zotta E & Ibarra C 2006 Cytotoxic effect of Shiga toxin-2 holotoxin and its B subunit on human renal tubular epithelial cells. *Microbes and Infection* **8** 410–419. (https://doi.org/10.1016/j.micinf.2005.07.005)

Forstermann U & Sessa WC 2012 Nitric oxide synthases: regulation and function. *European Heart Journal* **33** 829–837. (https://doi.org/10.1093/eurheartj/ehr304)

Giakoumelou S, Wheelhouse N, Cuschieri K, Entrican G, Howie SE & Horne AW 2016 The role of infection in miscarriage. *Human Reproduction Update* **22** 116–133. (https://doi.org/10.1093/humupd/dmv041)

Gibbs RS 2001 The relationship between infections and adverse pregnancy outcomes: an overview. *Annals of Periodontology* **6** 153–163. (https://doi.org/10.1902/annals.2001.6.1.153)

Graham CH, Hawley TS, Hawley RG, Macdougall JR, Kerbel RS, Khoo N & Lala PK 1993 Establishment and characterization of first trimester human trophoblast cells with extended lifespan. *Experimental Cell Research* **206** 204–211. (https://doi.org/10.1006/excr.1993.1139)

Hambartsoumian E, Srivastava RK & Seibel MM 2001 Differential expression and regulation of inducible nitric oxide synthase (iNOS) mRNA in human trophoblasts in vitro. *American Journal of Reproductive Immunology* **45** 78–85. (https://doi.org/10.1111/j.8755-8920.2001.450203.x)

Hussein HS 2007 Prevalence and pathogenicity of Shiga toxin-producing Escherichia coli in beef cattle and their products. *Journal of Animal Science* **85** E63–E72. (https://doi.org/10.2527/jas.2006-421)

Ibarra C, Amaral MM & Palermo MS 2013 Advances in pathogenesis and therapy of hemolytic uremic syndrome caused by Shiga toxin-2. *IUBMB Life* **65** 827–835. (https://doi.org/10.1002/iub.1206)

Karmali MA, Petric M, Lim C, Fleming PC, Arbus GS & Lior H 1985 The association between idiopathic hemolytic uremic syndrome and infection by verotoxin-producing Escherichia coli. *Journal of Infectious Diseases* **151** 775–782. (https://doi.org/10.1093/infdis/151.5.775)

Krause BJ, Hanson MA & Casanello P 2011 Role of nitric oxide in placental vascular development and function. *Placenta* **32** 797–805. (https://doi.org/10.1016/j.placenta.2011.06.025)

Lala PK & Chakraborty C 2003 Factors regulating trophoblast migration and invasiveness: possible derangements contributing to pre-eclampsia and fetal injury. *Placenta* **24** 575–587. (https://doi.org/10.1016/S0143-4004(03)00063-8)

Melton-Celsa AR 2014 Shiga toxin (Stx) classification, structure, and function. *Microbiology Spectrum* **2**. (https://doi.org/10.1128/microbiolspec.EHEC-0024-2013)

Muthing J, Schweppe CH, Karch H & Friedrich AW 2009 Shiga toxins, glycosphingolipid diversity, and endothelial cell injury. *Thrombosis and Haemostasis* **101** 252–264. (https://doi.org/10.1160/TH08-05-0317)

Obrig TG, Louise CB, Lingwood CA, Boyd B, Barley-Maloney L & Daniel TO 1993 Endothelial heterogeneity in Shiga toxin receptors and responses. *Journal of Biological Chemistry* **268** 15484–15488.

Peltier MR 2003 Immunology of term and preterm labor. *Reproductive Biology and Endocrinology* **1** 122. (https://doi.org/10.1186/1477-7827-1-122)

Sacerdoti F, Amaral MM, Zotta E, Franchi AM & Ibarra C 2014 Effects of Shiga toxin type 2 on maternal and fetal status in rats in the early stage of pregnancy. *BioMed Research International* **2014** 384645. (https://doi.org/10.1155/2014/384645)

Sacerdoti F, Amaral MM, Aisemberg J, Cymeryng CB, Franchi AM & Ibarra C 2015 Involvement of hypoxia and inflammation in early pregnancy loss mediated by Shiga toxin type 2. *Placenta* **36** 674–680. (https://doi.org/10.1016/j.placenta.2015.03.005)

Sacerdoti F, Scalise ML, Burdet J, Amaral MM, Franchi AM & Ibarra C 2018 Shiga toxin-producing Escherichia coli infections during pregnancy. *Microorganisms* **6**. (https://doi.org/10.3390/microorganisms6040111)

Sprague AH & Khalil RA 2009 Inflammatory cytokines in vascular dysfunction and vascular disease. *Biochemical Pharmacology* **78** 539–552. (https://doi.org/10.1016/j.bcp.2009.04.029)

Staun-Ram E & Shalev E 2005 Human trophoblast function during the implantation process. *Reproductive Biology and Endocrinology* **3** 56. (https://doi.org/10.1186/1477-7827-3-56)

Strasberg P, Grey A, Warren I & Skomorowski MA 1989 Simultaneous fractionation of four placental neutral glycosphingolipids with a continuous gradient. *Journal of Lipid Research* **30** 121–127.

Straszewski-Chavez SL, Abrahams VM, Alvero AB, Aldo PB, Ma Y, Guller Y, Romero R & Mor G 2009 The isolation and characterization of a novel telomerase immortalized first trimester trophoblast cell line, Swan. *Placenta* **30** 939–948. (https://doi.org/10.1016/j.placenta.2009.08.007)

Tang L, He G, Liu X & Xu W 2017 Progress in the understanding of the etiology and predictability of fetal growth restriction. *Reproduction* **153** R227–R240. (https://doi.org/10.1530/REP-16-0287)

Torres AG 2017 Escherichia coli diseases in Latin America-a 'one Health' multidisciplinary approach. *Pathogens and Disease* **75**. (https://doi.org/10.1093/femspd/ftx012)

Waddell T, Cohen A & Lingwood CA 1990 Induction of verotoxin sensitivity in receptor-deficient cell lines using the receptor glycolipid globotriosylceramide. *PNAS* **87** 7898–7901. (https://doi.org/10.1073/pnas.87.20.7898)

Received 12 November 2018
First decision 18 December 2018
Revised manuscript received 21 December 2018
Accepted 8 January 2019